European Journal of Medicinal Chemistry 46 (2011) 2786–2796

Contents lists available at ScienceDirect

European Journal of Medicinal Chemistry

journal homepage: http://www.elsevier.com/locate/ejmech

Original article

Synthesis, antiproliferative activity, and mechanism of action of a series of 2-{[(2*E*)-3-phenylprop-2-enoyl]amino}benzamides

Demetrio Raffa [a,*], Benedetta Maggio [a], Fabiana Plescia [a], Stella Cascioferro [a], Salvatore Plescia [a], Maria Valeria Raimondi [a], Giuseppe Daidone [a], Manlio Tolomeo [b], Stefania Grimaudo [b], Antonietta Di Cristina [b], Rosaria Maria Pipitone [b], Ruoli Bai [c], Ernest Hamel [c]

[a] *Dipartimento di Scienze e Tecnologie Molecolari e Biomolecolari, Via Archirafi, 32, 90123 Palermo, Italy*
[b] *Centro Interdipartimentale di Ricerca in Oncologia Clinica e Dipartimento Biomedico di Medicina Interna e Specialistica, Università di Palermo, Palermo, Italy*
[c] *Screening Technologies Branch, Developmental Therapeutics Program, Division of Cancer Treatment and Diagnosis, National Cancer Institute at Frederick, National Institutes of Health, Frederick, MD 21702, USA*

ARTICLE INFO

Article history:
Received 29 September 2010
Received in revised form
23 March 2011
Accepted 31 March 2011
Available online 6 April 2011

Keywords:
2-{[2*E*]-3-phenylprop-2-enoylamino}benzamides
Antimitotic agents
Cytotoxic activity

ABSTRACT

Several new 2-{[(2*E*)-3-phenylprop-2-enoyl]amino}benzamides **12a**–**s** and **17t**–**v** were synthesized by stirring in pyridine the (*E*)-3-(2-R1-3-R2-4-R3-phenyl)acrylic acid chlorides **11c**–**k** and **11t**–**v** with the appropriate anthranilamide derivatives **10a**–**c** or the 5-iodoanthranilic acid **13**. Some of the synthesized compounds were evaluated for their in vitro antiproliferative activity against the full NCI tumor cell line panel derived from nine clinically isolated cancer types (leukemia, non-small cell lung, colon, CNS, melanoma, ovarian, renal, prostate and breast). COMPARE analysis, effects on tubulin polymerization in cells and with purified tubulin, and effects on cell cycle distribution for **17t**, the most active of the series, indicate that these new antiproliferative compounds act as antitubulin agents.

© 2011 Elsevier Masson SAS. All rights reserved.

1. Introduction

During a screening program to find antiproliferative compounds in our laboratory's collection of small organic molecules, the 2-cinnamamido-5-iodobenzamide **1** was found at 10 μM to inhibit proliferation of the leukemic cell line K562 by 74%.

Compound **1** belongs to cinnamoyl anthranilates, which represent a class of biologically active substances of great importance in medicinal chemistry. Tranilast (Rizaben®) **2** is an antiallergic drug approved in 1982 for use in Japan and South Korea for bronchial asthma and was also investigated for use as an antiproliferative agent on drug-eluting stents. Its derivative (*E*)-2-(3-(3,4-dimethoxyphenyl)acrylamido)benzamide **3** [1] is another member of this class of compounds and is more potent than the lead compound, Tranilast (Fig. 1).

Other biological activities possessed by this class of compounds are antifibrotic and antinflammatory properties [2,3] and inhibition of cornea pterygium progression and blood vessel development [4,5]. Finally, cinnamoyl anthranilates are useful for prevention and treatment of glomerular diseases [6] and diseases caused by the excessive proliferation of vascular intimal cells [7].

However, despite their wide range of biological activities, a review of the literature revealed that no anticancer activity had been described for cinnamoyl anthranilates. Thus, the activity of compound **1** as an inhibitor of K562 proliferation led us to explore the potential of this class of compounds as anticancer agents, and we therefore synthesized a series of novel cinnamoyl anthranilates and screened the compounds for antileukemic activity. Our work enabled us to perform an initial study of their structure-activity relationships and to determine their mechanism of action. Compounds **12a**–**s** and **17t**–**v** were initially tested in vitro for their antileukemic activity against the K562 (human chronic myelogenous leukemia) cell line (Table 1). Among these, **12a**–**c** and **17t,u**, which showed the best antiproliferative activity, were selected by the National Cancer Institute (NCI) for evaluation in the 60 human tumor cell line screen of the NCI.

2. Results and discussion

2.1. Chemistry

A series of 2-{[(2*E*)-3-phenylprop-2-enoyl]amino}benzamides **12a**–**s** and **17t**–**v** was synthesized by stirring the (*E*)-3-(2-R1-3-R2-

* Corresponding author. Tel.: +39 91 23891917.
E-mail address: demraffa@unipa.it (D. Raffa).

0223-5234/$ – see front matter © 2011 Elsevier Masson SAS. All rights reserved.
doi:10.1016/j.ejmech.2011.03.067

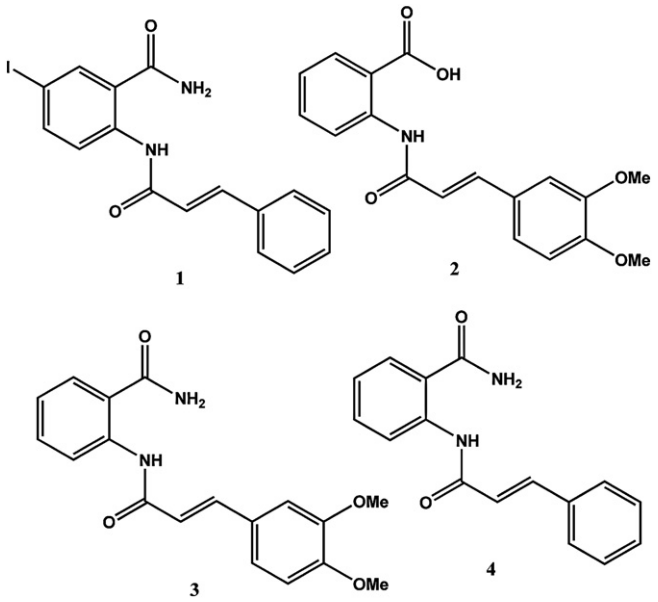

Fig. 1. Structure of cinnamoyl anthranilates.

4-R3-phenyl)acrylic acid chlorides **11c–k, 11t–v** and the appropriate anthranilamide derivatives **10a–c** or the 5-iodoanthranilic acid **13** as described in Schemes 1 and 2.

Crude (*E*)-3-(2-R1-3-R2-4-R3-phenyl)acrylic acids **11c–k**, **11t–v** were obtained by refluxing the appropriately substituted acrylic acid **8c–k**, **8t–v** with thionyl chloride. The 5-methylanthranilamide **10a** was obtained by reduction of 2-nitro-5-methylbenzamideamide **7a** as shown in Scheme 1. Compound **7** was obtained by reaction of the acid **5** with thionyl chloride to afford **6**, followed by treatment of **6** with aqueous ammonia.

The anthranilamide derivatives **10b,c** were obtained by stirring the appropriate 2*H*-3,1-benzoxazine-2,4(1*H*)-dione **9b,c** in aqueous ammonia solution (Scheme 1) [8].

A different synthetic method was used to obtain the 2-{[(2*E*)-3-phenylprop-2-enoyl]amino}benzamides **17t–v** (Scheme 2). The starting materials, 2-cinnamamido-5-iodobenzoic acids **15t–v**, were obtained by stirring the 5-iodoanthranilic acid **13** and the cinnamoyl chlorides **11t–v**. The reaction gave a mixture of (*E*)-6-iodo-2-styryl-4H-benzo[d] [1,3]oxazin-4-ones **14t–u** and 2-cinnamamido-5-iodobenzoic acids **15t–u**, and the mixtures were treated with aqueous Na_3PO_4 [9] to give the corresponding acids **15t** [10], **15u,v** as the only products. By treating the acids **15t–v** with ethyl chloroformate, the 2*H*-3,1-benzoxazine-2,4-diones **16t–v** were obtained [11], which, in turn, converted to the 2-{[2*E*]-3-phenylprop-2-enoylamino}benzamides **17t–v** by refluxing them in an aqueous ammonia solution [8].

Table 1
Percent growth inhibition obtained with the K562 cell line with compounds at 10 μM and IC_{50} values (μM) with the same cells.

Com.	% inhibition	**IC50** (μM)
4	14.2	>10
12a	65.4	5.5
12b	64.0	2.5
12c	62.4	5.0
12d	58.0	7.4
12e	28.2	>10
12f	31.0	>10
12g	49.0	10
12h	27.0	>10
12i	52.2	9.5
12j	37.8	>10
12k	64.0	6.3
12l	59.0	8.1
12m	25.5	>10
12n	22.0	>10
12o	46.2	>10
12p	45.9	>10
12q	43.2	>10
12r	43.8	>10
12s	45.9	>10
17t	74.5	0.57
17u	74.1	1.2
17v	26.3	>10
18	63.6	0.02

The structures of the new compounds were determined by analytical and spectroscopic measurements. In particular, ^{1}H NMR spectra of compounds **12a–s** and **17v–t** were consistent with an *E*-olefinic structure. They showed signals attributable to the β-olefinic protons at 6.66–6.97 δ with coupling constants of 16.6–14.7 Hz, as required for *E*-structures [12], while the α-olefinic hydrogens were found along with aromatic multiplets. Moreover, their ^{1}H NMR spectra showed both the NH and NH_2 amidic signals; the cinnamamido NH proton appeared as a singlet at 11.77–11.92 δ, while, according to the literature [13], the presence of an intramolecular hydrogen bond renders the benzamido NH_2 protons diastereotopic. H_a is easily exchangeable with D_2O and appeared as a singlet at 8.24–8.44 δ. H_b was found at a lower field along with the aromatic multiplets.

2.2. Biology

Synthesized 2-{[(2*E*)-3-phenylprop-2-enoyl]amino}benzamides **12a–s** and **17t–v** were initially tested in vitro for their antileukemic activity against the K562 (human chronic myelogenous leukemia) cell line. Colchicine **18**, whose antileukemic activity is well known, and the 2-cinnamamidobenzamide **4** [13] (Fig. 1), were used as reference compounds. The percent growth inhibition at a screening concentration of 10 μM and the IC_{50} values for compounds that exhibited at least 50% of growth inhibition at 10 μM are shown in Table 1. Compounds **12a–s** and **17t–v** had inhibitory activity against the K562 cells ranging from 22.0 to 74.5% at 10 μM, with **12a–d**, **12k,l**, and **17t,u** (IC_{50} 0.57–8.1 μM) being the most active compounds. Our data (Table 1) showed positive effects following substitution with halogens at the 5 position of the benzamido moiety, especially when the substituent was iodine (compounds **17t** and **17u**). As far as structure-activity relationships are concerned, it seems that the introduction of a substituent in both the benzamido and styryl moieties are favorable for inhibition of K562 cell growth relative to the unsubstituted 2-cinnamamidobenzamide **4** (Table 1). However, the best activity was obtained when the substitutions were present only on the benzamido moiety (compounds **12a–d, 17t**). Compounds substituted in both the benzamido and styryl moieties (compounds **12e–s**, **17v**) were less active, even if antiproliferative activity was maintained in the ortho-styryl derivatives (**12d,i,l,u**).

Compounds **12a**, **12b**, **12c**, **17t** and **17u** were evaluated by the NCI for testing against a panel of approximately 60 human cell lines derived from seven clinically isolated cancer types (lung, colon, melanoma, renal, ovarian, brain, and leukemia) according to the NCI standard protocol [14] (Table 2). The data summarized in Table 2 showed that **12a**, **12b**, **12c**, **17t** and **17u** caused 50% growth inhibition at micromolar (**12a**, **12b**, **12c**) and submicromolar concentrations (**17t**, **17u**) against every type of tumor cell line investigated.

Moreover, a mean graph midpoint (MG_MID) is calculated for the GI50, TGI and LC50 parameters, giving an average activity parameter for all the cell lines. For the calculation of the MG_MID, insensitive cell lines are included and assigned as their values the highest concentration tested. Considering the MG_MID values

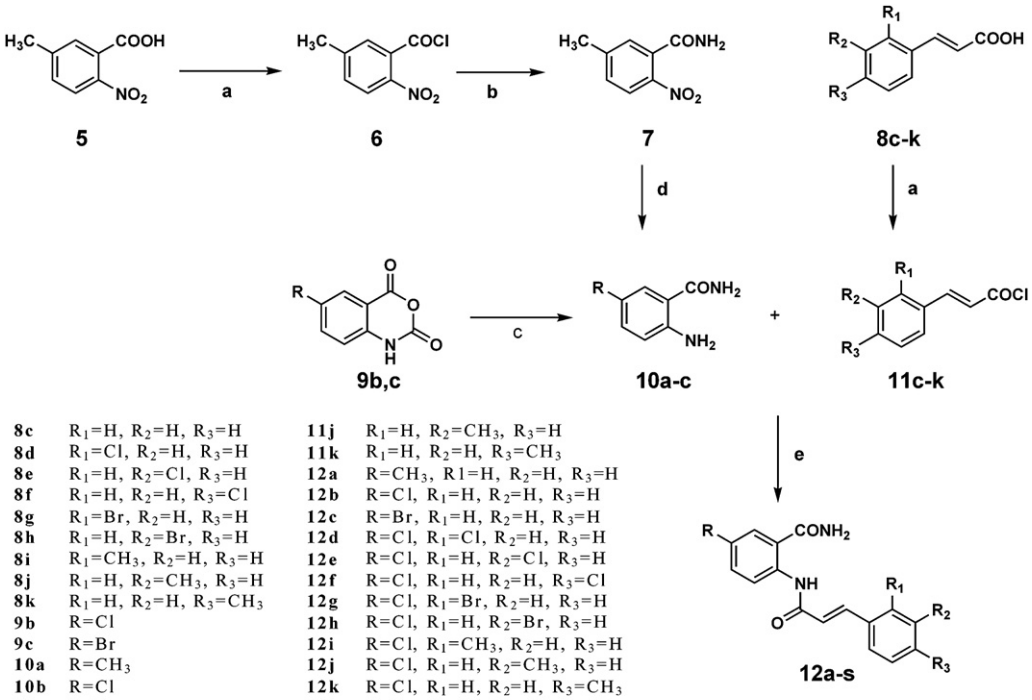

8c	R_1=H, R_2=H, R_3=H	**11j**	R_1=H, R_2=CH_3, R_3=H
8d	R_1=Cl, R_2=H, R_3=H	**11k**	R_1=H, R_2=H, R_3=CH_3
8e	R_1=H, R_2=Cl, R_3=H	**12a**	R=CH_3, R1=H, R_2=H, R_3=H
8f	R_1=H, R_2=H, R_3=Cl	**12b**	R=Cl, R_1=H, R_2=H, R_3=H
8g	R_1=Br, R_2=H, R_3=H	**12c**	R=Br, R_1=H, R_2=H, R_3=H
8h	R_1=H, R_2=Br, R_3=H	**12d**	R=Cl, R_1=Cl, R_2=H, R_3=H
8i	R_1=CH_3, R_2=H, R_3=H	**12e**	R=Cl, R_1=H, R_2=Cl, R_3=H
8j	R_1=H, R_2=CH_3, R_3=H	**12f**	R=Cl, R_1=H, R_2=H, R_3=Cl
8k	R_1=H, R_2=H, R_3=CH_3	**12g**	R=Cl, R_1=Br, R_2=H, R_3=H
9b	R=Cl	**12h**	R=Cl, R_1=H, R_2=Br, R_3=H
9c	R=Br	**12i**	R=Cl, R_1=CH_3, R_2=H, R_3=H
10a	R=CH_3	**12j**	R=Cl, R_1=H, R_2=CH_3, R_3=H
10b	R=Cl	**12k**	R=Cl, R_1=H, R_2=H, R_3=CH_3
10c	R=Br	**12l**	R=Br, R_1=Cl, R_2=H, R_3=H
11c	R_1=H, R_2=H, R_3=H	**12m**	R=Br, R_1=H, R_2=Cl, R_3=H
11d	R_1=Cl, R_2=H, R_3=H	**12n**	R=Br, R_1=H, R_2=H, R_3=Cl
11e	R_1=H, R_2=Cl, R_3=H	**12°**	R=Br, R_1=Br, R_2=H, R_3=H
11f	R_1=H, R_2=H, R_3=Cl	**12p**	R=Br, R_1=H, R_2=Br, R_3=H
11g	R_1=Br, R_2=H, R_3=H	**12q**	R=Br, R_1=CH_3, R_2=H, R_3=H
11h	R_1=H, R_2=Br, R_3=H	**12r**	R=Br, R_1=H, R_2=CH_3, R_3=H
11i	R_1=CH_3, R_2=H, R_3=H	**12s**	R=Br, R_1=H, R_2=H, R_3=CH_3

Scheme 1. Reagents and conditions: (a) $SOCl_2$, reflux, 5 h; (b) acetonitrile, aqueous ammonia (25%), reflux, 8 h; (c) aqueous ammonia (25%), stirring, rt, 1 h; (d) $SnCl_2$, HCl (35%), stirring, 0–5 °C, (24 h); (e) pyridine, stirring, rt, 24 h.

(Table 3), the most active compound of the series was derivative **17t**, at both the GI50 and TGI levels, followed by **17u** and **12c**.

Compound **17t** was selected by the NCI for evaluation in its vivo toxicity assay, with the finding that the compound was nontoxic at a dose of 400 mg/kg in nontumored mice. Compound **17t** was also selected by the NCI for testing in the hollow fiber assay, a preliminary in vivo screening tool, but the compound was not sufficiently active for evaluation in xenograft models.

To predict the probable mechanism of action, the NCI's bioinformatic tool COMPARE analysis [15] was performed for the most active compound **17t**. When tested as seed against the NCI "standard agents" Database, the compound showed Pearson Correlation Coefficients (PCC) of 0.492 and 0.476 at the GI50 level and higher values, 0.677, 0.600, 0.597, at the TGI level. In all cases the highest PCC's were with compounds NSC 332598 (rhizoxin), NSC 125973 (paclitaxel), NSC 49842 (vinblastine sulfate) and NSC 153858 (maytansine), which are all antimitotic agents directed against tubulin.

To verify the prediction of the COMPARE algorithm, the effects of **17t** on cell cycle distribution as determined by flow cytometry and on tubulin polymerization were evaluated.

As shown in Fig. 2, **17t** caused a dose dependant increase of K562 cells in the G2-M phase of the cell cycle and a decrease of cells in G0-G1 after a 24 h treatment. This is the typical flow cytometric cell cycle distribution observed with drugs targeting tubulin (see panel b in Fig. 2), which is the main component of the mitotic spindle.

After 48 h **17t** caused extensive apoptosis in K562 cells, with an AC50 (concentration inducing 50% apoptosis) of 3.7 μM (Fig. 3). Apoptosis in this experiment was measured as described in the Experimental Section.

To confirm the ability of **17t** to act on microtubules, the percentage of cells blocked in mitosis (M) was morphologically determined after staining cells with ethidium bromide and acridine orange. The percentage of K562 cells blocked in the M phase after 24 h of exposure to 1 μM **17t** was 35 ± 6 (Fig. 4A, untreated K562 cell as control <1%). Of interest, concentrations of **17t** higher than 2 μM induced morphologic alterations in almost all treated cells, suggesting an interaction between **17t** and the cytoskeleton of K562 cells (Fig. 4C and D).

To examine the effects of **17t** on microtubules (tubulin) and microfilaments (actin), PtK2 cells were examined by direct immunofluorescence. These cells were selected for this examination since their flattened morphology yields high quality images of cytoskeletal elements, particularly the microtubule and microfilament networks. As shown in Fig. 5, the microtubules disappeared while the microfilaments persisted with micromolar **17t**. In addition, we found that **17t** partially inhibited the polymerization of purified tubulin, but this effect was relatively weak, as shown in Fig. 6, with a comparison to the much stronger inhibition observed with colchicine **18**. With **17t**, we observed a concentration dependent inhibition of the rate of microtubule assembly, beginning at about 10 μM. However, within the concentration range we were able to examine (up to 40 μM), there was no effect on the extent of assembly. It should be pointed out that **17t** appeared to partially precipitate at 40 μM. With the classic antitubulin agent colchicine **18**, the rate of assembly was 50% inhibited at about 2 μM, and the extent of assembly at about 5 μM. At 7 and 10 μM colchicine **18**, tubulin polymerization was essentially completely inhibited, an effect that we were unable to achieve with **17t**.

Taken together, our data suggest that **17t** interacts with tubulin, preventing formation of the mitotic spindle and thereby caused

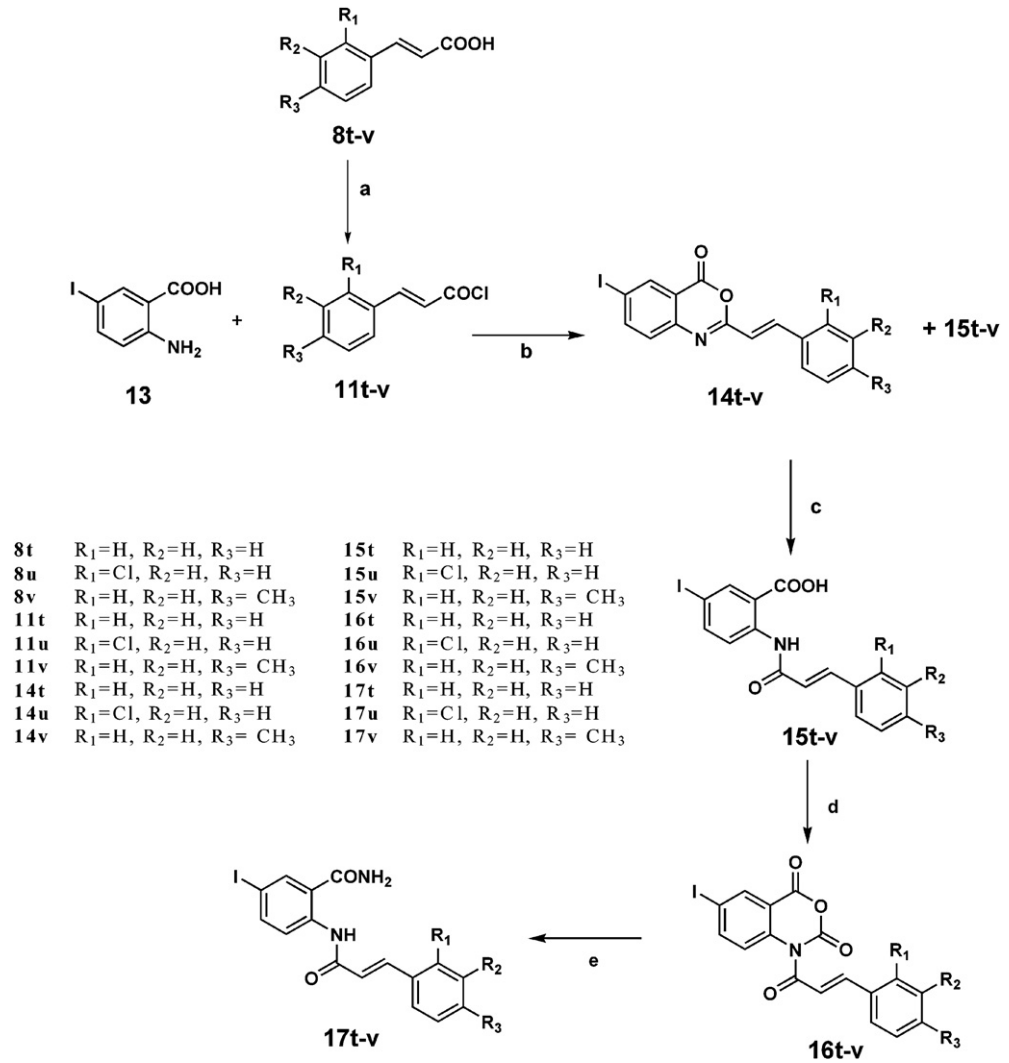

Scheme 2. Reagents and conditions: (a) $SOCl_2$, reflux, 5 h; (b) pyridine, stirring, 0–5 °C, 24 h; (c) aqueous $NaPO_3$ (0.01 M), reflux, 20 h; (d) ethyl chloroformate, acetyl chloride reflux, (15 min + 30 min); (e) dioxane, acqueous ammonia (25%), reflux, 3 h.

the block in M phase. Inhibition of tubulin assembly would also disrupt the integrity of the microtubule cytoskeleton in interphase cells, causing extensive alterations in cell morphology. Although its effect on in vitro tubulin assembly is relatively weak, the cellular effects obtained with **17t** are most consistent with those observed with more potent antitubulin agents. Furthermore, disruption of cellular microtubules invariably results in activation of cellular apoptosis.

3. Conclusions

The data reported here show that the 2-{[2*E*]-3-phenylprop-2-enoylamino}benzamides **12a**–**s** and **17t**–**v** caused growth inhibition against many tumor cell lines. The best agents inhibited proliferation at low micromolar (**12a**, **12b**, **12c**) and submicromolar concentrations (**17t**, **17u**) against every tumor cell line investigated. The best activity was obtained when the 5 position of the benzamido moiety was substituted with an iodine atom. COMPARE analysis, effects on tubulin polymerization in cells and with purified tubulin, and effects on cell cycle distribution, including induction of apoptosis, indicate that these new antiproliferative compounds act as antitubulin agents.

4. Experimental

4.1. Chemistry

4.1.1. General

Reaction progress was monitored by TLC on silica gel plates (Merck 60, F_{254}, 0.2 mm). Organic solutions were dried over Na_2SO_4. Evaporation refers to the removal of solvent on a rotary evaporator under reduced pressure. All melting points were determined on a Büchi 530 capillary melting point apparatus and are uncorrected. IR spectra were recorded with a Perkin Elmer Spectrum RXI FT-IR System spectrophotometer, with compound as a solid in a KBr disc. ^1H NMR spectra were obtained using a Bruker AC-E 300 MHz spectrometer (tetramethylsilane as internal standard): chemical shifts are expressed in δ values (ppm). Merck silica gel (Kiesegel 60/230–400 mesh) was used for flash chromatography columns. Microanalyses data (C, H, N) were obtained by an Elemental Vario EL III apparatus and were within ±0.4% of the theoretical values. Yields refer to purified products and are not optimized. The names of the products were obtained using the ACD/I-Lab Web service (ACD/IUPAC Name Free 8.05).

Table 2
Results of multi-dose growth inhibition assay (GI50, μM).

Cell line		12a	12b	12c	17t	17u
Leukemia	CCRF-CEM	2.36	2.96	0.429	0.341	0.484
	HL-60 (TB)	1.77	1.42	0.346	0.0542	0.165
	K-562	1.11	0.845	0.415	0.920	0.370
	MOLT-4	3.56	3.95	1.86	0.202	1.42
	RPMI-8226	nt	2.79	1.03	0.347	0.772
Non-small cell lung cancer	A549/ATCC	5.81	3.77	1.02	2.65	1.87
	EKVX	5.18	2.83	2.41	0.734	1.00
	HOP-62	7.74	3.15	1.51	0.800	2.30
	HOP-92	11.4	2.87	1.96	21.2	13.2
	NCI-H226	7.28	3.00	2.61	1.09	1.14
	NCI-H23	3.38	3.37	1.09	0.840	1.39
	NCI-H460	3.59	1.76	0.662	0.453	0.479
	NCI-H522	2.83	2.08	nt	0.303	0.459
Colon cancer	COLO 205	1.84	1.68	0.917	0.343	0.797
	HCC-2998	6.45	0.487	nt	1.25	0.984
	HCT-116	3.20	1.98	0.663	0.430	0.509
	HCT-15	3.77	2.13	1.04	0.586	0.987
	HT29	2.31	1.94	0.527	0.367	0.376
	KM12	2.94	1.69	0.739	0.499	0.533
	SW-620	3.30	1.99	0.705	0.541	0.605
CNS cancer	SF-268	10.9	2.90	1.83	2.31	0.778
	SF-295	3.14	1.40	0.625	0.350	0.415
	SF539	2.05	2.05	0.819	0.445	0.444
	SNB-19	5.69	3.18	2.00	0.586	1.41
	SNB75	3.18	1.84	2.07	0.245	1.22
	U251	4.13	2.14	0.887	0.501	0.663
Melanoma	LOX IMVI	7.65	4.33	3.27	3.75	4.21
	MALME-3M	7.59	2.68	1.21	1.60	nt
	M14	2.35	1.71	0.482	0.429	0.698
	MDA-MB-435	0.660	0.492	0.231	nt	0.234
	SK-MEL-2	4.75	2.75	nt	1.40	0.678
	SK-MEL-28	5.24	2.88	0.839	2.51	nt
	SK-MEL-5	1.01	0.373	0.435	0.383	0.367
	UACC-257	17.0	15.1	nt	14.3	38.7
	UACC-62	3.77	2.52	0.782	0.632	0.388
Ovarian cancer	IGROV1	4.37	3.29	1023	0.917	0.352
	OVCAR-3	2.18	1.30	0.349	0.353	0.294
	OVCAR-4	11.4	2.77	nt	1.84	2.37
	OVCAR-5	8.20	2.74	2.92	3.52	4.02
	OVCAR-8	7.49	3.89	nt	1.06	56.0
	NCI/ADR-RES	2.79	2.24	0.400	nt	0.719
	SK-OV-3	2.79	2.30	1.41	0.744	0.539
Renal cancer	786–0	4.00	2.32	1.76	1.43	0.937
	A498	5.56	3.61	1.70	2.70	0.880
	ACHN	13.5	4.75	3.36	3.70	9.86
	CAKI-1	8.92	0.263	1.34	0.648	0.637
	RXF 393	nt	1.71	0.444	3.02	0.425
	SN12C	9.63	3.96	2.96	0.635	1.55
	TK-10	25.8	5.51	2.67	3.15	26.7
	UO-31	9.62	3.57	1.85	3.53	1.63
Prostate cancer	PC-3	3.97	3.15	0.684	0.628	0.832
	DU-145	3.66	2.16	0.935	0.477	1.28
Breast cancer	MCF7	3.48	1.74	0.569	0.450	0.401
	MDA-MB-231	7.26	2.48	2.19	0.596	1.41
	HS 578T	1.94	2.04	0.624	0.375	0.362
	BT-549	4.88	3.19	1.41	9.47	0.816
	T-47D	4.20	3.36	1.57	0.857	19.9
	MDA-MB-468	3.12	1.17	0.279	nt	0.377

nt = not tested.
GI50 = Growth inhibition of 50%; [(Ti−Tz)/(C−Tz)] × 100 = 50 where Tz = absorbance at $t = 0$, Ti = absorbance at $t = 48$ h, C = absorbance of control at $t = 48$ h.

4.1.2. General procedure for preparation of 5-methyl-2-nitrobenzoyl chloride *6a* and 3-phenylacryloyl chlorides *11c–k*, *11t–v*

Substituted benzoyl and acryloyl chlorides **6a**, **11c–k** and **11t–v** were obtained by refluxing for 5 h the appropriate acid derivatives **5a, 8c–k** and **8t–v** (0.01 mol) with thionyl chloride (7.25 ml) [16]. After evaporation under reduced pressure, the crude liquid residue was used for subsequent reactions without purification.

4.1.3. Preparation of 5-methyl-2-nitrobenzamide *7a*

To 0.01 mol of 5-methyl-2-nitrobenzoyl chloride **6a** 10 ml of aqueous ammonia solution (25%) and 33 ml of acetonitrile were added. The solution was first refluxed for 8 h, then evaporated under reduced pressure to give pure **7a**.

4.1.4. Preparation of 5-methyl-2-aminobenzamide *10a*

To a magnetically stirred suspension of stannous chloride (0.038 mol) in concentrated HCl (37%) (15 ml), 0.013 mole of **7a** was added at a rate so that the temperature of the slurry was maintained below 5 °C (about 1 h). After addition was complete, the mixture was stirred for 24 h. The white slurry thus obtained was diluted with cold water (150 ml), and aqueous sodium hydroxide (40%) was added until the tin salt dissolved. The solution was extracted with ethyl acetate (3 × 150 ml), and the extracts dried and evaporated *in vacuo* to obtain pure **10a**.

4.1.5. General procedure for preparation of aminobenzamides *10b,c*

A mixture of 0.01 mol of 2*H*-3,1-benzoxazine-2,4(1*H*)-diones **9b,c** and 25 ml of aqueous ammonia solution (25%) was stirred for 1 h. The solid precipitate was removed by filtration, washed with an aqueous ammonia solution (5%) and crystallized from ethanol.

4.1.6. General procedure for preparation of 2-{[(2E)-3-phenylprop-2-enoyl]amino}benzamides *12a–s*

To a cold (0–5 °C) stirred suspension of aminobenzamides **10a–c** (0.016 mol) in pyridine (13 ml), 0.016 mol of the appropriate 3-phenylacryloyl chloride **11c–k** was added over 30 min. After addition was complete, the solution was stirred for 24 h and then poured onto crushed ice. The precipitate was removed by filtration, washed with water, and crystallized from ethanol.

5-Methyl-2-{[(2E)-3-phenylprop-2-enoyl]amino}benzamide (**12a**): yield 85%; mp 228–230 °C (dioxane); I.R. (KBr) cm^{-1} 3400-3258 (NH, NH_2), 1681, 1651 (2XCO); ^1H NMR (DMSO) δ 2.31 (s, 3H, CH_3); 6.89 (d, 1H, $J = 15.6$ Hz, olefinic CH); 7.32–8.49 (a set of signals, 9H, aromatic protons and NH-H); 7.58 (d, 1H, $J = 15.6$ Hz, olefinic CH); 8.24 (s, 1H, NH–H, exchangeable); 11.80 (s, 1H, NH, exchangeable). Anal. ($C_{17}H_{16}N_2O_2$) C,H,N

5-Chloro-2-{[(2E)-3-phenylprop-2-enoyl]amino}benzamides (**12b**): yield 67%; mp 218–220 °C (dioxane); I.R. (KBr) cm^{-1} 3384, 3218 (NH, NH_2), 1682, 1659 (2XCO); ^1H NMR (DMSO) δ 6.83 (d, 1H, $J = 14.9$ Hz, olefinic CH); 7.43–8.63 (a set of signals, 10H, aromatic protons, olefinic CH and NH–H); 8.42 (s, 1H, NH–H, exchangeable); 11.82 (s, 1H, NH, exchangeable). Anal. ($C_{16}H_{13}ClN_2O_2$) C,H,N

5-Bromo-2-{[(2E)-3-phenylprop-2-enoyl]amino}benzamides (**12c**): yield 98%; mp 229–231 °C (dioxane); I.R. (KBr) cm^{-1} 3388, 3217 (NH, NH_2), 1682, 1659 (2XCO); ^1H NMR (DMSO) δ 6.82 (d, 1H, $J = 14.9$ Hz, olefinic CH); 7.43–8.58 (a set of signals, 10H, aromatic protons, olefinic CH and NH–H); 8.44 (s, 1H, NH–H, exchangeable); 11.84 (s, 1H, NH, exchangeable). Anal. ($C_{16}H_{13}BrN_2O_2$) C,H,N

5-Chloro-2-{[(2E)-3-(2-chlorophenyl)prop-2-enoyl]amino}benzamides (**12d**): yield 36%; mp 268–270 °C (dioxane); I.R. (KBr) cm^{-1} 3365, 3155 (NH, NH_2), 1686, 1661 (2XCO); ^1H NMR (DMSO) δ 6.90 (d, 1H, $J = 15.2$ Hz olefinic CH); 7.38–8.63 (a set of signals, 9H, aromatic protons, olefinic CH and NH–H); 8.43 (s, 1H, NH–H, exchangeable); 11.92 (s, 1H, NH, exchangeable). Anal. ($C_{16}H_{12}Cl_2N_2O_2$) C,H,N

5-Chloro-2-{[(2E)-3-(3-chlorophenyl)prop-2-enoyl]amino}benzamides (**12e**): yield 88%; mp 260–261 °C (dioxane); I.R. (KBr) cm^{-1} 3351, 3157 (NH, NH_2), 1681, 1662 (2XCO); ^1H NMR (DMSO) δ 6.97 (d, 1H, $J = 16.6$ Hz, olefinic CH); 7.45–8.63 (a set of signals, 9H, aromatic protons, olefinic CH and NH–H); 8.42 (s, 1H, NH–H, exchangeable); 11.79 (s, 1H, NH, exchangeable). Anal. ($C_{16}H_{12}Cl_2N_2O_2$) C,H,N

Table 3
Overview of the results of the in vitro antitumor screening for compounds **12a–c** and **17t,u**.[a]

Comp	no. Studied[e]	pGI50[b]			pTGI[c]			pLC50[d]		
		no. giving positive results[e]	range	MG_MID[f]	no. giving positive results[e]	range	MG_MID[f]	no. giving positive results[e]	range	MG_MID[f]
12a	58	58	6.18–4.59	5.36	30	5.53–4.00	4.31	2	4.44–4.00	4.01
12b	58	58	6.58–4.82	5.65	29	6.06–4.00	4.53	7	5.19–4.00	4.06
12c	52	52	6.64–5.47	5.99	23	6.18–4.00	4.58	10	5.02–4.00	4.07
17t	59	59	7.27–4.67	6.05	44	6.41–4.00	4.71	17	4.94–4.00	4.10
17u	57	57	6.78–4.41	5.97	32	6.17–4.00	4.62	8	4.90–4.00	4.05

[a] Data obtained from the NCI's in vitro disease-oriented human tumor cells screen.
[b] pGI50 is the −log of the molar concentration that inhibits 50% net cell growth.
[c] pTGI is the −Log of the molar concentration giving total growth inhibition.
[d] pLC50 is the −Log of the molar concentration leading to 50% net cell death.
[e] Refers to the number of cell lines.
[f] MG_MID = mean graph midpoint = arithmetical mean value for all tested cancer cell lines. If the indicated effect was not attainable within the used concentration interval, the highest tested concentration was used for the calculation.

5-Chloro-2-{[(2E)-3-(4-chlorophenyl)prop-2-enoyl]amino}benzamides (**12f**): yield 58%; mp 243–244 °C (dioxane); I.R. (KBr) cm^{-1} 3356, 3283, 3177 (NH, NH_2), 1675, 1661 (2XCO); ^1H NMR (DMSO) δ 6.87 (d, 1H, J = 14.9 Hz, olefinic CH); 7.47–8.62 (a set of signals, 9H, aromatic protons, olefinic CH and NH–H). 8.43 (s, 1H, NH–H, exchangeable); 11.82 (s, 1H, NH, exchangeable). Anal. ($C_{16}H_{12}Cl_2N_2O_2$) C,H,N

2-{[(2E)-3-(2-bromophenyl)prop-2-enoyl]amino}benzamides (**12g**): yield 66%; mp 261–262 °C (dioxane); I.R. (KBr) cm^{-1} 3366, 3157 (NH, NH_2), 1686, 1662 (2XCO); ^1H NMR (DMSO) δ 6.87 (d, 1H, J = 14.8 Hz, olefinic CH); 7.35–8.63 (a set of signals, 9H, aromatic protons, olefinic CH and NH–H); 8.43 (s, 1H, NH–H, exchangeable); 11.90 (s, 1H, NH, exchangeable). Anal. ($C_{16}H_{12}BrClN_2O_2$) C,H,N

2-{[(2E)-3-(3-bromophenyl)prop-2-enoyl]amino}benzamides (**12h**): yield 91%; mp 251–252 °C (dioxane); I.R. (KBr) cm^{-1} 3349, 3167 (NH, NH_2), 1678, 1662 (2XCO); ^1H NMR (DMSO) δ 6.96 (d, 1H, J = 15.1 Hz, olefinic CH); 7.34–8.64 (a set of signals, 9H, aromatic protons, olefinic CH and NH–H); 8.43 (s, 1H, NH–H, exchangeable); 11.80 (s, 1H, NH, exchangeable). Anal. ($C_{16}H_{12}BrClN_2O_2$) C,H,N

5-Chloro-2-{[(2E)-3-(2-methylphenyl)prop-2-enoyl]amino}benzamides (**12i**): yield 42%; mp 231–232 °C (dioxane); I.R. (KBr) cm^{-1} 3383, 3165 (NH, NH_2), 1687, 1660 (2XCO); ^1H NMR (DMSO) δ 2.34 (s, 3H, CH_3); 6.66 (d, 1H, J = 15.6 Hz, olefinic CH); 7.28–8.42 (a set of signals, 9H, aromatic protons, olefinic CH and NH–H); 8.42 (s, 1H, NH–H, exchangeable); 11.89 (s, 1H, NH, exchangeable). Anal. ($C_{17}H_{15}ClN_2O_2$) C,H,N

5-Chloro-2-{[(2E)-3-(3-methylphenyl)prop-2-enoyl]amino}benzamides (**12j**): yield 82%; mp 238–239 °C (dioxane); I.R. (KBr) cm^{-1} 3337, 3163 (NH, NH_2), 1681, 1660 (2XCO); ^1H NMR (DMSO) δ 2.34 (s, 3H, CH_3); 6.80 (d, 1H, J = 15.4 Hz, olefinic CH); 7.21–8.65 (a set of signals, 9H, aromatic protons, olefinic CH and NH–H); 8.43 (s, 1H, NH–H, exchangeable); 11.83 (s, 1H, NH, exchangeable). Anal. ($C_{17}H_{15}ClN_2O_2$) C,H,N

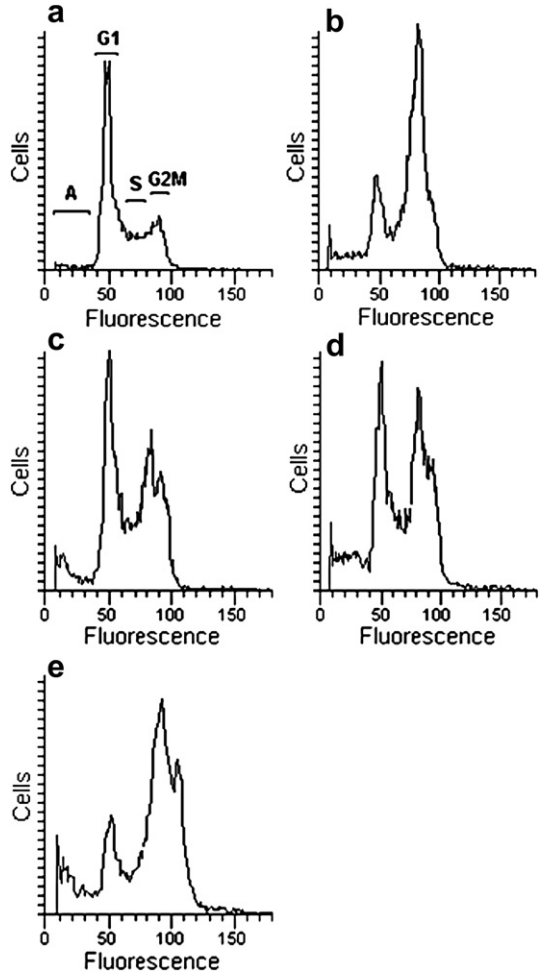

Fig. 2. Effects of compound **17t** on DNA content/cell following treatment of K562 cells for 24 h. The cells were cultured without compound (control, a), with an antimitotic drug used as internal standard (60 nM taxol (b)) and with 1 μM (c), 2 μM (d), or 4 μM (e) **17t**. Cell cycle distribution was analyzed by the standard propidium iodide procedure as described in Materials and Methods. Sub-G0–G1 (A), G0–G1, S, and G2-M cells are indicated in (a).

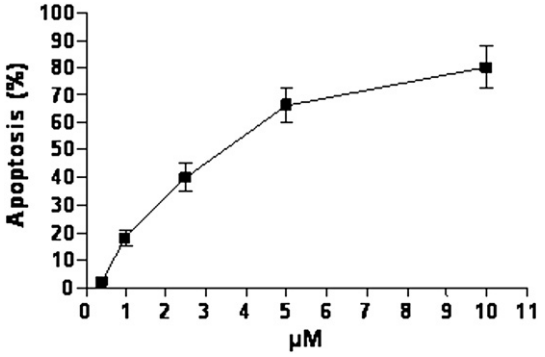

Fig. 3. Percentage of apoptosis induced by compound **17t** in K562 cells. Cells were cultured with different concentrations of **17t**. Apoptosis was evaluated after 48 h of treatment as described in the experimental section. Bars: ±SE.

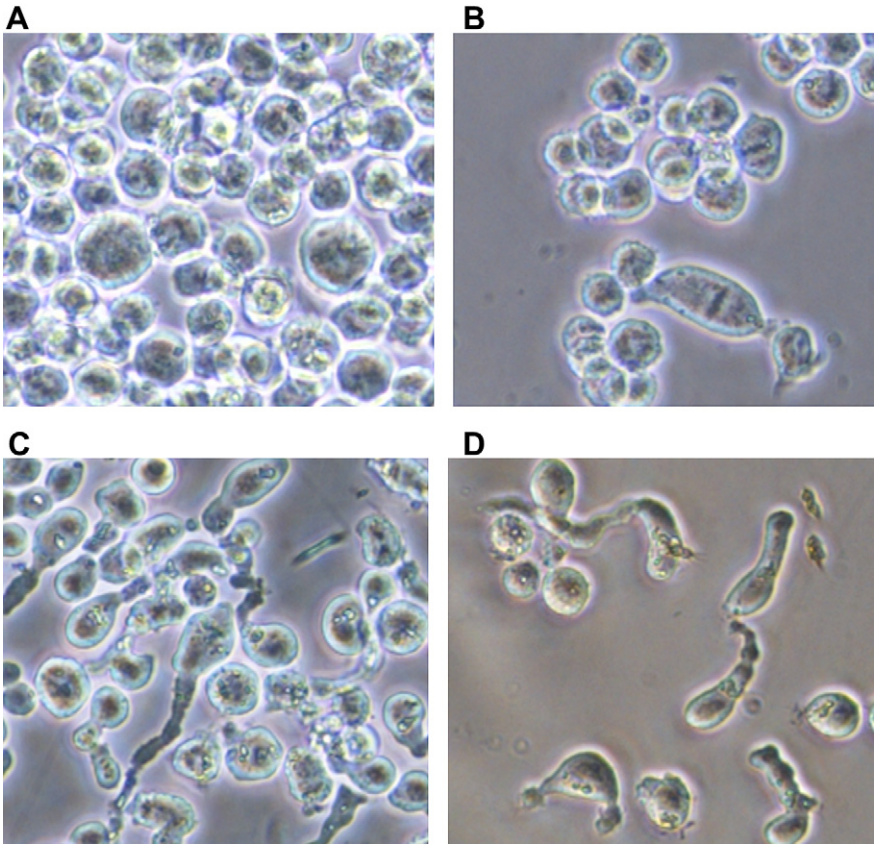

Fig. 4. Morphology of K562 cells after 24 h exposure to 2 μM (B), 5 μM (C) and 10 μM (D) compound **17t**. (A) Untreated K562 cells (control). Living cells in culture medium were observed by using a phase contrast invertoscope (40× magnification).

5-Chloro-2-{[(2E)-3-(4-methylphenyl)prop-2-enoyl]amino}benzamides (**12k**): yield 82%; mp 238–239 °C (dioxane); I.R. (KBr) cm^{-1} 3379, 3212 (NH, NH_2), 1682, 1660 (2XCO); ^1H NMR (DMSO) δ 2.34 (s, 3H, CH_3); 6.78 (d, 1H, J = 15.2 Hz, olefinic CH); 7.23–8.62 (a set of signals, 9H, aromatic protons, olefinic CH and NH–H); 8.43 (s, 1H, NH–H, exchangeable); 11.77 (s, 1H, NH, exchangeable). Anal. ($C_{17}H_{15}ClN_2O_2$) C,H,N

5-Bromo-2-{[(2E)-3-(2-chlorophenyl)prop-2-enoyl]amino}benzamides (**12l**): yield 73%; mp 250–251 °C (dioxane); I.R. (KBr) cm^{-1} 3366, 3153 (NH, NH_2), 1685, 1661 (2XCO); ^1H NMR (DMSO) δ 6.91 (d, 1H, J = 15.1 Hz, olefinic CH); 7.42–8.02 (a set of signals, 9H, aromatic protons, olefinic CH and NH–H); 8.42 (s, 1H, NH–H, exchangeable); 11.90 (s, 1H, NH, exchangeable). Anal. ($C_{16}H_{12}BrClN_2O_2$) C,H,N

5-Bromo-2-{[(2E)-3-(3-chlorophenyl)prop-2-enoyl]amino}benzamides (**12m**): yield 56%; mp 260–261 °C (dioxane); I.R. (KBr) cm^{-1} 3352, 3154 (NH, NH_2), 1680, 1662 (2XCO); ^1H NMR (DMSO) δ 6.97 (d, 1H, J = 16.0 Hz, olefinic CH); 7.45–8.58 (a set of signals, 9H, aromatic protons, olefinic CH and NH–H); 8.44 (s, 1H, NH–H, exchangeable); 11.81 (s, 1H, NH, exchangeable). Anal. ($C_{16}H_{12}BrClN_2O_2$) C,H,N

5-Bromo-2-{[(2E)-3-(4-chlorophenyl)prop-2-enoyl]amino}benzamides (**12n**): yield 57%; mp 255–256 °C (dioxane); I.R. (KBr) cm^{-1} 3357, 3285, 3178 (NH, NH_2), 1673, 1660 (2XCO); ^1H NMR (DMSO) δ 6.87 (d, 1H, J = 14.7 Hz, olefinic CH); 7.47–8.55 (a set of signals, 9H, aromatic protons, olefinic CH and NH–H); 8.42 (s, 1H, NH–H, exchangeable); 11.79 (s, 1H, NH, exchangeable). Anal. ($C_{16}H_{12}BrClN_2O_2$) C,H,N

5-Bromo-2-{[(2E)-3-(2-bromophenyl)prop-2-enoyl]amino}benzamides (**12o**): yield 81%; mp 258–259 °C (dioxane); I.R. (KBr) cm^{-1} 3366, 3153 (NH, NH_2), 1685, 1661 (2XCO); ^1H NMR (DMSO) δ 6.87 (d, 1H, J = 16.5 Hz, olefinic CH); 7.71–8.52 (a set of signals, 9H, aromatic protons, olefinic CH and NH–H); 8.42 (s, 1H, NH–H, exchangeable); 11.88 (s, 1H, NH, exchangeable). Anal. ($C_{16}H_{12}Br_2N_2O_2$) C,H,N

5-Bromo-2-{[(2E)-3-(3-bromophenyl)prop-2-enoyl]amino}benzamides (**12p**): yield 81%; mp 258–259 °C (dioxane); I.R. (KBr) cm^{-1} 3348, 3156 (NH, NH_2), 1678, 1661 (2XCO); ^1H NMR (DMSO) δ 6.97 (d, 1H, J = 15.6 Hz, olefinic CH); 7.35–8.56 (a set of signals, 9H, aromatic protons, olefinic CH and NH–H); 8.43 (s, 1H, NH–H, exchangeable); 11.78 (s, 1H, NH, exchangeable). Anal. ($C_{16}H_{12}Br_2N_2O_2$) C,H,N

5-Bromo-2-{[(2E)-3-(2-methylphenyl)prop-2-enoyl]amino}benzamides (**12q**): yield 98%; mp 238–240 °C (dioxane); I.R. (KBr) cm^{-1} 3384, 3160 (NH, NH_2), 1686, 1659 (2XCO); ^1H NMR (DMSO) δ 2.32 (s, 3H, CH_3); 6.74 (d, 1H, J = 15.4 Hz, olefinic CH); 7.25–8.56 (a set of signals, 9H, aromatic protons, olefinic CH and NH–H); 8.42 (s, 1H, NH–H, exchangeable); 11.89 (s, 1H, NH, exchangeable). Anal. ($C_{17}H_{15}BrN_2O_2$) C,H,N

5-Bromo-2-{[(2E)-3-(3-methylphenyl)prop-2-enoyl]amino}benzamides (**12r**): yield 71%; mp 268–270 °C (dioxane); I.R. (KBr) cm^{-1} 3338, 3163 (NH, NH_2), 1681, 1661 (2XCO); ^1H NMR (DMSO) δ 2.34 (s, 3H, CH_3); 6.80 (d, 1H, J = 16.5 Hz, olefinic CH); 7.24–8.63 (a set of signals, 9H, aromatic protons, olefinic CH and NH–H); 8.42 (s, 1H, NH–H, exchangeable); 11.80 (s, 1H, NH, exchangeable). Anal. ($C_{17}H_{15}BrN_2O_2$) C,H,N

5-Bromo-2-{[(2E)-3-(4-methylphenyl)prop-2-enoyl]amino}benzamides (**12s**): yield 88%; mp 236–237 °C (dioxane); I.R. (KBr) cm^{-1} 3353, 3163 (NH, NH_2), 1678, 1660 (2XCO); ^1H NMR (DMSO) δ 2.33 (s, 3H, CH_3); 6.75 (d, 1H, J = 14.8 Hz, olefinic CH); 7.22–8.56 (a set of

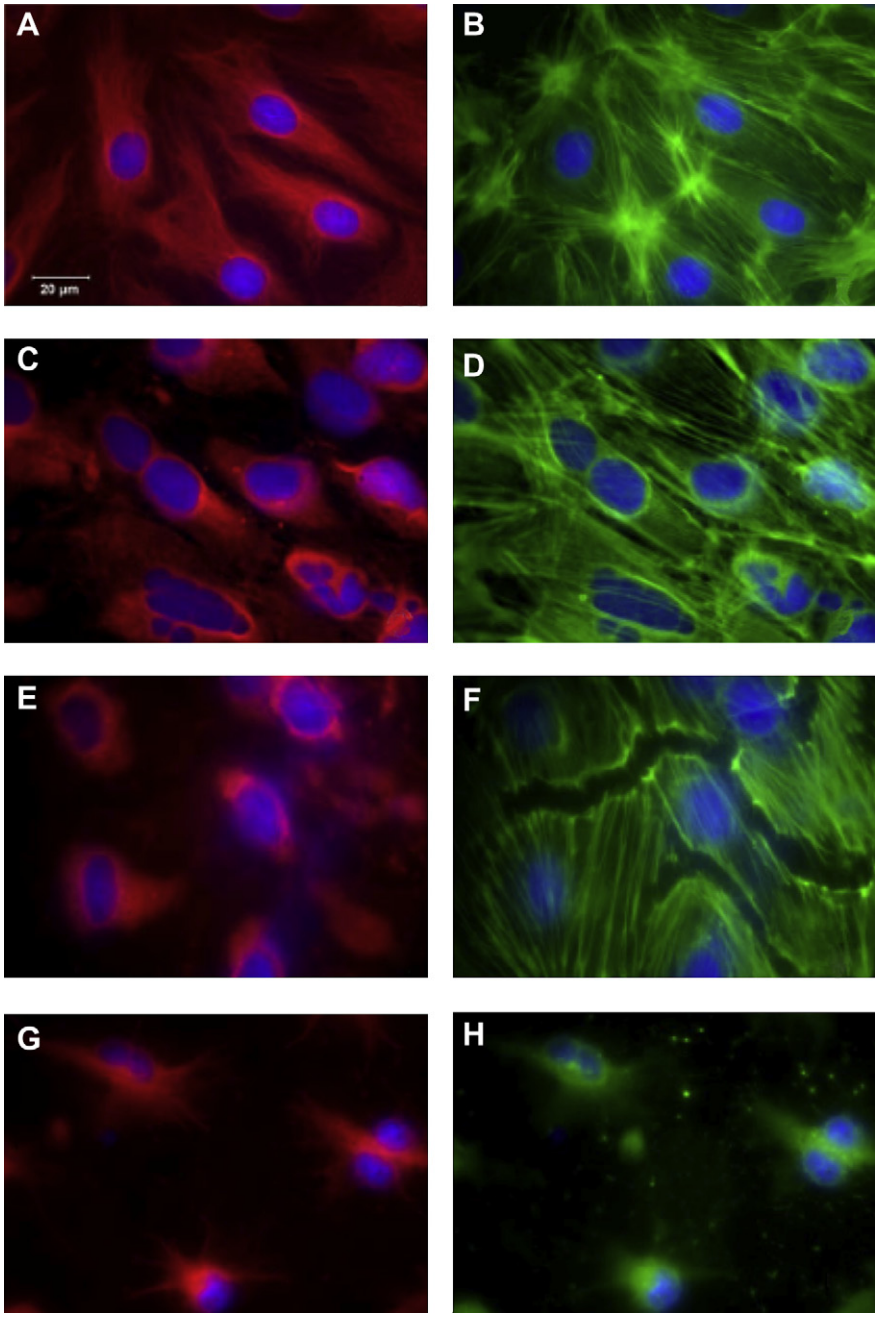

Fig. 5. Panels A, C, E, and G, PtK2 cells stained for tubulin with an antibody to β-tubulin conjugated to Cy3. Panels B, D, F, and H, PtK2 cells stained for actin with an antibody to β-actin conjugated to FTIC. A and B, untreated cells. C and D, cells treated with 10 μM **17t**. E and F, cells treated with 1 μM combretastatin A-4 (a potent antitubulin drug). G and H, cells treated with 1 μM latrunculin A (a potent inhibitor of actin assembly).

signals, 9H, aromatic protons, olefinic CH and NH–H); 8.42 (s, 1H, NH–H, exchangeable); 11.78 (s, 1H, NH, exchangeable). Anal. ($C_{17}H_{15}BrN_2O_2$) C,H,N

*4.1.7. General procedure for preparation of 2-cinnamamido-5-iodobenzoic acids **15t–v***

To an ice cooled (0–5 °C) stirred solution of 2-amino-5-iodobenzoic acid **13** (3 mmol) in anhydrous pyridine (20 ml) 2 mmol of cinnamoyl chlorides **11t–v** was added. The solution was left stirring overnight, then poured into cold water. The precipitate was collected as a mixture of (*E*)-6-iodo-2-styryl-4H-benzo[d] [1,3] oxazin-4-ones **14t–u** and 2-cinnamamido-5-iodobenzoic acids **15t–v**. The mixture was refluxed in 0.01 M aqueous Na_3PO_4 for 20 h. The solution was allowed to cool to room temperature and, after filtration, was acidified with HCl (0.1 M) to pH 2 to give the corresponding acids **15t** [10] and **15u** as the only products. Finally, the precipitate was removed by filtration and washed with cold chloroform to obtain pure **15t,u**. In the case of cinnamoyl chloride **11v**, treatment with 2-amino-5-iodobenzoic acid **13** (3 mmol) in anhydrous pyridine (20 ml) directly gave pure (*E*)-5-iodo-2-(3-*o*-tolylacrylamido)benzoic acid **15v**.

(E)-2-(3-(2-chlorophenyl)acrylamido)-5-iodobenzoic acid (**15u**): yield 80%; mp 250–252 °C (ethanol); I.R. (KBr) cm^{-1} 3448, 3117 (NH, OH), 1703, 1688 (2XCO); ^1H NMR (DMSO) δ 6.94 (d, 1H,

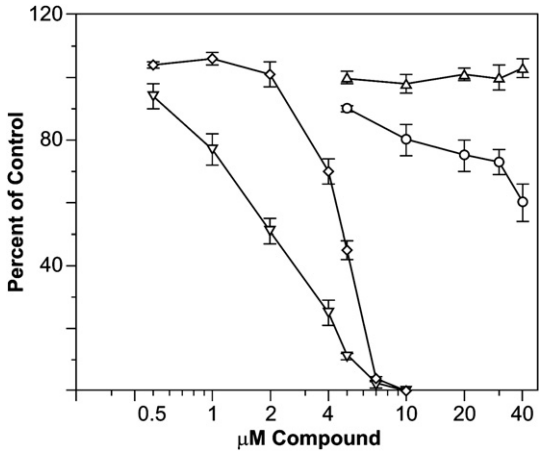

Fig. 6. Comparison of the effects of **17t** with those of colchicine as an inhibitor of the polymerization of purified tubulin. Assembly was followed in Gilford model 250 recording spectrophotometers equipped with electronic temperature controllers. Reaction mixtures were preincubated at 30 °C without GTP and chilled on ice. GTP (0.4 mM) was added to the samples, which were transferred to cuvettes held at 0 °C. Baselines were established, and the temperature was jumped to 30 °C over about 60 s and held there for 20 min. Maximal reaction rates and extent of assembly were determined for each sample and compared to a control reaction mixture in the same experiment. Each data point was obtained in triplicate, and standard deviations are shown. Symbols as follows: o, maximum rates obtained with **17t**; Δ, extents of reaction obtained with **17t**; ∇, maximum rates obtained with colchicine; ◇, extents of reaction obtained with colchicine.

J = 15.3 Hz, olefinic CH); 7.44–8.43 (a set of signals, 8H, aromatic protons, olefinic CH); 11.37 (s, 1H, NH–H, exchangeable); 13.98 (s, 1H, OH, exchangeable). Anal. ($C_{16}H_{11}ClINO_3$) C,H,N

(E)-5-iodo-2-(3-o-tolylacrylamido)benzoic acid (**15v**): yield 83%; mp 239–240 °C (ethanol); I.R. (KBr) cm^{-1} 3353, 3163 (NH, NH_2), 1678, 1660 (2XCO); ^{1}H NMR (DMSO) δ 2.37 (s, 3H, CH_3); 6.82 (d, 1H, J = 15.3 Hz, olefinic CH); 7.27–8.48 (a set of signals, 8H, aromatic protons, olefinic CH); 11.28 (s, 1H, NH–H, exchangeable); 13.90 (s, 1H, OH, exchangeable). Anal. ($C_{17}H_{14}INO_3$) C,H,N

4.1.8. General procedure for preparation of 6-iodo-1H-benzo[d] [1,3]oxazine-2,4-diones *16t–v*

A mixture of 2-cinnamamido-5-iodobenzoic acids **15t–v** (4.6 mmol) and ethylchloroformate (25 ml) was refluxed for 15 min. After this time, acetyl chloride (1.5 ml) was added, and reflux continued for an additional 30 min. On cooling, the product precipitated, was removed by filtration, and was washed with chloroform to give pure **16t–v**. Compound **16v** easily decomposed and was used as is without purification.

1-Cinnamoyl-6-iodo-1H-benzo[d] [1,3] oxazine-2,4-dione (**16t**): yield 83%; mp 201–204 °C ($CHCl_3$); I.R. (KBr) cm^{-1} 1760, 1670 (3XCO); ^{1}H NMR (DMSO) δ 6.96 (d, 1H, J = 16 Hz, olefinic CH); 7.39–8.42 (a set of signals, 9H, aromatic protons and olefinic C). Anal. ($C_{17}H_{10}INO_4$) C,H,N

(E)-1-(3-(2-chlorophenyl)acryloyl)-6-iodo-1H-benzo[d] [1,3]oxazine-2,4-dione (**16u**): yield 83%; mp 201–204 °C ($CHCl_3$); I.R. (KBr) cm^{-1} 1760, 1660 (3XCO); ^{1}H NMR (DMSO) δ 7.01 (d, 1H, J = 16 Hz, olefinic CH); 7.38–8.33 (a set of signals, 8H, aromatic protons and olefinic C). Anal. ($C_{17}H_9ICINO_4$) C,H,N

4.1.9. General procedure for preparation of 2-cinnamamido-5-iodobenzamides *17t-v*

A solution of 6-iodo-1H-benzo[d] [1,3]oxazine-2,4-diones **16t–v** (2.3 mmol), 25% aqueous ammonia solution (28 ml) and dioxane (5 ml) was left under reflux for 3 h. After this time, the solution was kept in a freezer to allow the product to precipitate. It was removed by filtration and crystallized from dioxane.

5-iodo-2-{[(2E)-3-phenylprop-2-enoyl]amino}benzamide (**17t**): yield 88%; mp 260–261 °C (dioxane); I.R. (KBr) cm^{-1} 3393, 3215 (NH, NH_2), 1680, 1656 (2XCO); ^{1}H NMR (DMSO) δ 6.82 (d, 1H, J = 15.6 Hz, olefinic CH); 7.43–8.42 (a set of signals, 10H, aromatic protons, olefinic CH and NH–H); 8.15 (s, 1H, NH–H, exchangeable); 11.80 (s, 1H, NH, exchangeable). Anal. ($C_{16}H_{13}IN_2O_2$) C,H,N

5-Iodo-2-{[(2E)-3-(2-chlorophenyl)prop-2-enoyl]amino}benzamides (**17u**): yield 88%; mp 260–261 °C (dioxane); I.R. (KBr) cm^{-1} 3381, 3155 (NH, NH_2), 1681, 1660 (2XCO); ^{1}H NMR (DMSO) δ 6.97 (d, 1H, J = 16.6 Hz, olefinic CH); 7.45–8.63 (a set of signals, 9H, aromatic protons, olefinic CH and NH–H); 8.42 (s, 1H, NH–H, exchangeable); 11.79 (s, 1H, NH, exchangeable). Anal. ($C_{16}H_{12}ClIN_2O_2$) C,H,N

5-iodo-2-{[(2E)-3-(2-methylphenyl)prop-2-enoyl]amino}benzamide (**17v**): yield 88%; mp 260–261 °C (dioxane); I.R. (KBr) cm^{-1} 3368, 3294, 3192 (NH, NH_2), 1673, 1658 (2XCO); ^{1}H NMR (DMSO) δ 2.34 (s, 3H, CH_3); 6.97 (d, 1H, J = 16.6 Hz, olefinic CH); 7.45–8.63 (a set of signals, 9H, aromatic protons, olefinic CH and NH–H); 8.14 (s, 1H, NH–H, exchangeable); 11.77 (s, 1H, NH, exchangeable). Anal. ($C_{17}H_{15}IN_2O_2$) C,H,N

4.2. Biology

4.2.1. Antiproliferative activity

Compounds **12a–s** and **17t–v** were initially tested in vitro for antiproliferative activity against the K562 (human chronic myelogenous leukemia) cell line. These cell lines were grown at 37 °C in a humidified atmosphere containing 5% CO_2, in RPMI-1640 medium supplemented with 10% fetal bovine serum and antibiotics.

K562 cells were suspended at a density of 1×10^5 cells/ml in growth medium, transferred to a 24-well plate (1 ml/well), cultured with or without (in the case of control wells) a screening concentration of 10 μM compounds and incubated at 37 °C for 48 h. Numbers of viable cells were determined by counting in a hematocytometer after dye exclusion with trypan blue [17]. The antiproliferative effects of the compounds were estimated in terms of % growth inhibition, comparing cell viability of treated and untreated cells. We determined IC50 values (test agent concentration at which the cell proliferation was inhibited by 50% as compared with the untreated control) for compounds that exhibited the best activity at the screening concentration.

4.2.2. Tumor cell line screening

The in vitro antiproliferative activity values were obtained by the Developmental Therapeutics Program, National Cancer Institute (USA) [18]

The human tumor cell lines of the cancer screening panel are grown in RPMI 1640 medium containing 5% fetal bovine serum and 2 mM L-glutamine. For a typical screening experiment, cells are inoculated into 96 well microtiter plates in 100 μl at plating densities ranging from 5000 to 40,000 cells/well, depending on the doubling time of the individual cell lines. After cell inoculation, the microtiter plates are incubated at 37 °C, 5% CO_2, 95% air and 100% relative humidity for 24 h prior to addition of experimental drugs. After 24 h, two plates of each cell line are fixed *in situ* with TCA, to represent a measurement of the cell population for each cell line at the time of drug addition (Tz). Experimental drugs are solubilized in dimethyl sulfoxide at 400-fold the desired final maximum test concentration and stored frozen prior to use. At the time of drug addition, an aliquot of frozen concentrate is thawed and diluted to twice the desired final maximum test concentration with complete medium containing 50 μg/ml gentamicin. Additional four, 10-fold or ½ log serial dilutions are made to provide a total of five drug concentrations plus control. Aliquots of 100 μl of these different drug dilutions are added to the appropriate microtiter wells already containing 100 μl of medium, resulting in the required final drug

concentrations. Following drug addition, the plates are incubated for an additional 48 h at 37 °C, 5% CO_2, 95% air, and 100% relative humidity. For adherent cells, the assay is terminated by the addition of cold TCA. Cells are fixed *in situ* by the gentle addition of 50 μl of cold 50% (w/v) TCA (final concentration, 10% TCA) and incubated for 60 min at 4 °C. The supernatant is discarded, and the plates are washed five times with tap water and air dried. Sulforhodamine B (SRB) solution (100 μl) at 0.4% (w/v) in 1% acetic acid is added to each well, and plates are incubated for 10 min at room temperature. After staining, unbound dye is removed by washing five times with 1% acetic acid, and the plates are air dried. Bound stain is subsequently solubilized with 10 mM trizma base, and the absorbance is read on an automated plate reader at a wavelength of 515 nm. For suspension cells, the methodology is the same except that the assay is terminated by fixing settled cells at the bottom of the wells by gently adding 50 μl of 80% TCA (final concentration, 16% TCA). Using the seven absorbance measurements [time zero (Tz), control growth (C), and test growth in the presence of drug at the five concentration levels (Ti)], the percentage growth is calculated at each of the drug concentration levels. Percentage growth inhibition is calculated as:

$$[(\mathrm{Ti} - \mathrm{Tz})/(\mathrm{C} - \mathrm{Tz})] \times 100 \text{ for concentrations for which } \mathrm{Ti} \geq \mathrm{Tz}$$

$$[(\mathrm{Ti} - \mathrm{Tz})/\mathrm{Tz}] \times 100 \text{ for concentrations for which } \mathrm{Ti} < \mathrm{Tz}$$

Three dose response parameters are calculated for each experimental agent. Growth inhibition of 50% (GI_{50}) is calculated from [(Ti−Tz)/(C−Tz)] × 100 = 50, which is the drug concentration resulting in a 50% reduction in the net protein increase (as measured by SRB staining) in control cells during the drug incubation. The drug concentration resulting in total growth inhibition (TGI) is calculated from Ti = Tz. The LC_{50} (concentration of drug resulting in a 50% reduction in the measured protein at the end of the drug treatment as compared to that at the beginning) indicating a net loss of cells following treatment is calculated from [(Ti−Tz)/Tz] × 100 = −50. Values are calculated for each of these three parameters if the level of activity is reached; however, if the effect is not reached or is exceeded, the value for that parameter is expressed as greater or less than the maximum or minimum concentration tested.

4.2.3. Cytotoxicity assays

To evaluate the number of live and dead neoplastic cells, the cells were stained with trypan blue and counted on a hemocytometer. To determine the growth inhibitory activity of the drugs tested, 2×10^5 cells were plated into 25 mm wells (Costar, Cambridge, UK) in 1 ml of complete medium and treated with different concentrations of each drug. After 48 h of incubation, the number of viable cells was determined and expressed as percent of control proliferation.

4.2.4. Morphological evaluation of apoptosis

Drug induced apoptosis was determined morphologically after labeling with acridine orange and ethidium bromide. Cells (2 × 105) were centrifuged (300 × g), and the pellet was resuspended in 25 μl of the dye mixture. Ten μl of the mixture was examined under oil immersion with a 100× objective using a fluorescence microscope. Live cells were determined by the uptake of acridine orange (green fluorescence) and exclusion of ethidium bromide (red fluorescence) stain. Live and dead apoptotic cells were identified by perinuclear condensation of chromatin stained by acridine orange (100 μg/ml) or ethidium bromide (100 μg/ml), respectively, and by the formation of apoptotic bodies. The percentage of apoptotic cells was determined after counting at least 300 cells.

4.2.5. Determination of apoptosis by annexin-V

Cells (1×10^6) were washed with phosphate-buffered saline (PBS) and centrifuged at 200 × g for 5 min. Cell pellets were suspended in 100 μl of staining solution containing FITC-conjugated annexin-V and propidium iodide (Annexine-V-Fluos Staining Kit, Roche Molecular Biochemicals, Mannheim, Germany) and incubated for 15 min at 20 °C. Annexin-V positive cells were evaluated by flow cytometry (Becton−Dickinson.

4.2.6. Flow cytometric analysis of cell cycle and apoptosis

Cells were washed once in ice-cold PBS and resuspended at 1×10^6 ml in a hypotonic fluorochrome solution containing propidium iodide (Sigma) 50 μg/ml in 0.1% sodium citrate plus 0.03% (v/v) nonidet P-40 (Sigma). After 30 min of incubation, the fluorescence of each sample was analyzed as a single-parameter frequency histogram using a FACScan flow cytometer (Becton−Dickinson, San Jose, CA). Distribution of cells in the cell cycle was determined using the ModFit LT program (Verity Software House, Inc.). Apoptosis was determined by evaluating the percentage of hypodiploid nuclei accumulated in the sub-G0−G1 peak after labeling with propidium iodide.

4.2.7. Immunofluorescence

PtK2 cells (*Potorus tridactylis* kidney epithelial cells) were obtained from the American Type Tissue Collection and grown as recommended by the supplier. The technique was described in detail previously [19,20]. Cells were treated with compounds for 24 h at 37 °C prior to fixation and staining with antibodies (Cy3 conjugate of anti-β-tubulin clone TUB2.1 and FTIC conjugate of anti-β-actin clone Ac-15 monoclonal antibodies from Sigma). Cells were examined with a Nikon Eclipse E800 microscope equipped with epifluorescence and appropriate filters, and images were collected with a Spot digital camera.

4.2.8. Tubulin assembly

The procedure with purified bovine brain tubulin was described in detail previously [21].

Acknowledgment

Financial support from MIUR (40% funding) is gratefully acknowledged. The authors wish to thank the Developmental Therapeutics Program of the National Cancer Institute of the United States of America for performing the antiproliferative screening of compounds.

References

[1] H. Ogita, Y. Isobe, H. Takaku, R. Sekine, Y. Goto, S. Misawa, H. Hayashi, Bioorg. Med. Chem. Lett. 11 (2001) 549−551.
[2] S.J. Williams, D. Stapleton, S. Zammit, D.J. Kelly, R.E. Gilbert, H., Krum, Patent WO2008003141 (2008); Chem. Abst. 148:144415.
[3] Y. Bo, P.P. Chakrabarti, N. Chen, E.M. Doherty, C.H. Fotsch, N. Han, M.G. Kelly, Q. Liu, M.H. Norman, X. Wang, J. Zhu, Ognynanov, V., Patent WO03049702 (2003); Chem. Abst. 139:53025.
[4] H. Harada, M. Isaji, H. Miyata, H. Kusama, Y. Nonaka, K. Kamata, T. Yazaki, Hotei, Y., Patent JP10330254 (1998); Chem. Abst. 130:105331.
[5] H. Harada, M. Isaji, H. Kusama, Y. Taketana, Y. Nonaka, T. Kamata, Y. Futai, Patent JP10259129 (1998); Chem. Abst. 129:321163.
[6] H. Harada, H. Kusama, Y. Nonaka, K. Kamata, Y. Fotei, Patent JP10360124 (1998); Chem. Abst. 130:47477.
[7] H. Harada, H. Kusama, Y. Nonaka, K. Kamata, Y. Hotei, A. Iyobe, H. Fujikura, F. Satoh, Patent WO9709301 (1997); Chem. Abst. 126:250990.
[8] A.V. Dolzhenco-Podchezertseva, L.M. Korkodinova, M.V. Vasilyuc, V.P. Kotegov, Pharm. Chem. J. 36 (2002) 647−648.

[9] K. Bratt, K. Sunnerheim, S. Bryngelsson, A. Fagerlund, L. Engman, R.E. Andersson, L.H. Dimberg, J. Agr. Food Chem. 51 (2003) 594–600.
[10] P. Rani, V.K. Srivastava, A. Kumar, Ind. J. Chem. B. Org. 42B (2003) 1729–1733.
[11] G.M. Coppola, Synthesis 7 (1980) 505–536.
[12] S. Chimichi, F. De Sio, D. Donati, G. Fina, R. Pepino, P. Sarti-Fantoni, Heterocycles 20 (1983) 263–267.
[13] J. Hanusek, M. Sedlák, P. Šimůnek, V. Štěrba, Eur. J. Org. Chem. 11 (2002) 1855–1863.
[14] M.R. Boyd, K.D. Paull, Drug Dev. Res. 34 (1995) 91–109.
[15] K.D. Paull, C.M. Lin, L. Malspeis, E. Hamel, Cancer Res. 52 (1992) 3892–3900.
[16] M.H. Palmer, G.J. McVie, J. Chem. Soc. B (1968) 745–751.
[17] S. Manfredini, R. Bazzanini, P.G. Baraldi, M. Guarneri, D. Simoni, M.E. Marongiu, A. Pani, P. La Colla, E. Tramontano, J. Med. Chem. 35 (1992) 917–924.
[18] The methodology can be found at http://dtp.nci.nih.gov/.
[19] R. Bai, P. Verdier-Pinard, S. Gangwar, C.C. Stessman, K.J. McClure, E.A. Sausville, G.R. Pettit, R.B. Bates, E. Hamel, Mol. Pharmacol. 59 (2001) 462–469.
[20] Z. Cruz-Monserrate, H.C. Vervoort, R. Bai, D.J. Newman, S.B. Howell, G. Los, J.T. Mullaney, M.D. Williams, G.R. Pettit, W. Fenical, E. Hamel, Mol. Pharmacol. 63 (2003) 1273–1280.
[21] E. Hamel, Cell Biochem. Biophys. 38 (2003) 1–22.